JCB Article

Mammalian PAR-1 determines epithelial lumen polarity by organizing the microtubule cytoskeleton

David Cohen,[1] Patrick J. Brennwald,[2] Enrique Rodriguez-Boulan,[1] and Anne Müsch[1]

[1]Margaret M. Dyson Vision Research Institute, Weill Medical College of Cornell University, New York, NY 10021
[2]Department of Cell and Developmental Biology, University of North Carolina, Chapel Hill, NC 27599

Epithelial differentiation involves the generation of luminal surfaces and of a noncentrosomal microtubule (MT) network aligned along the polarity axis. Columnar epithelia (e.g., kidney, intestine, and Madin-Darby canine kidney [MDCK] cells) generate apical lumina and orient MT vertically, whereas liver epithelial cells (hepatocytes and WIFB9 cells) generate lumina at cell–cell contact sites (bile canaliculi) and orient MTs horizontally. We report that knockdown or inhibition of the mammalian orthologue of *Caenorhabditis elegans* Par-1 (EMK1 and MARK2) during polarization of cultured MDCK and WIFB9 cells prevented development of their characteristic lumen and nonradial MT networks. Conversely, EMK1 overexpression induced the appearance of intercellular lumina and horizontal MT arrays in MDCK cells, making EMK1 the first known candidate to regulate the developmental branching decision between hepatic and columnar epithelial cells. Our experiments suggest that EMK1 primarily promotes reorganization of the MT network, consistent with the MT-regulating role of this gene product in other systems, which in turn controls lumen formation and position.

Introduction

A hallmark of the morphogenesis of nonstratified epithelia is the generation of luminal domains at characteristic locations. Columnar epithelia (e.g., kidney, intestine, or pancreas) display their lumina at the cell apex, separated by tight junctions from lateral domains enriched in cell–cell adhesion molecules and opposite to basal domains enriched in receptors for the extracellular matrix. In contrast, hepatic epithelial cells establish their lumina, the bile canaliculi (BC), at sites of intercellular contact separated by tight junctions from basolateral domains specialized for cell–cell interactions and exchange with the bloodstream (sinusoidal membranes). Although progress has been made identifying genes and mechanisms involved in lumen formation during tubulogenesis in cultured cell models and genetic organism models (for review see Hogan and Kolodziej, 2002; Zegers et al., 2003), no genes or mechanisms have been identified that contribute to the developmental decision to build an epithelium with columnar or hepatic lumen polarity.

A good candidate cellular system to regulate lumen position in epithelial cells is the microtubule (MT) cytoskeleton because of the following: (a) epithelial polarization is accompanied by a dramatic change in MT organization; (b) simple columnar epithelia have a MT organization that is different from that of hepatic epithelia; (c) the polarized delivery of apical (luminal) membrane proteins is controlled by the MT cytoskeleton (for review see Mays et al., 1994; Grindstaff et al., 1998; Kreitzer et al., 2003); and (d) MT disruption inhibits the maintenance of luminal domains in intestinal cells in vivo (Achler et al., 1989) and in the intestinal epithelial cell line Caco2 (Gilbert et al., 1991) and follicle formation in three-dimensional primary thyroid cultures (Yap and Manley, 2001). Nonpolarized epithelial cells exhibit a radial MT array with the slow-growing minus ends emanating from a juxtanuclear MT organizing center (MTOC) and the plus ends extending to the cell cortex (Bacallao et al., 1989), an arrangement generally observed in fibroblasts and other nonepithelial cells. When simple epithelial cells (e.g., MDCK) reach confluency and polarize, the MTs form vertical arrays with the negative ends facing an MTOC under the cell apex and arrays of mixed polarity at the apical and basal poles (Bacallao et al., 1989; Bre et al., 1990). Most MTs appear not to be associated with the MTOC; the mechanisms involved in release of MT negative ends from the MTOC and capture

The online version of this article includes supplemental material.

Address correspondence to Anne Müsch, Margaret M. Dyson Vision Research Institute, Weill Medical College of Cornell University, 1300 York Ave., Box 233, New York, NY 10021. Tel.: (212) 746-2260. Fax: (212) 746-8101. email: amuesch@mail.med.conell.edu

Key words: EMK1; MARK2; MDCK; WIFB; apical surface

Abbreviations: BC, bile canaliculi; DPPIV, dipeptidyl aminopeptidase IV; KN-EMK1, kinase-negative EMK1; MT, microtubule; MTOC, MT organizing center; VAC, vacuolar apical compartment.

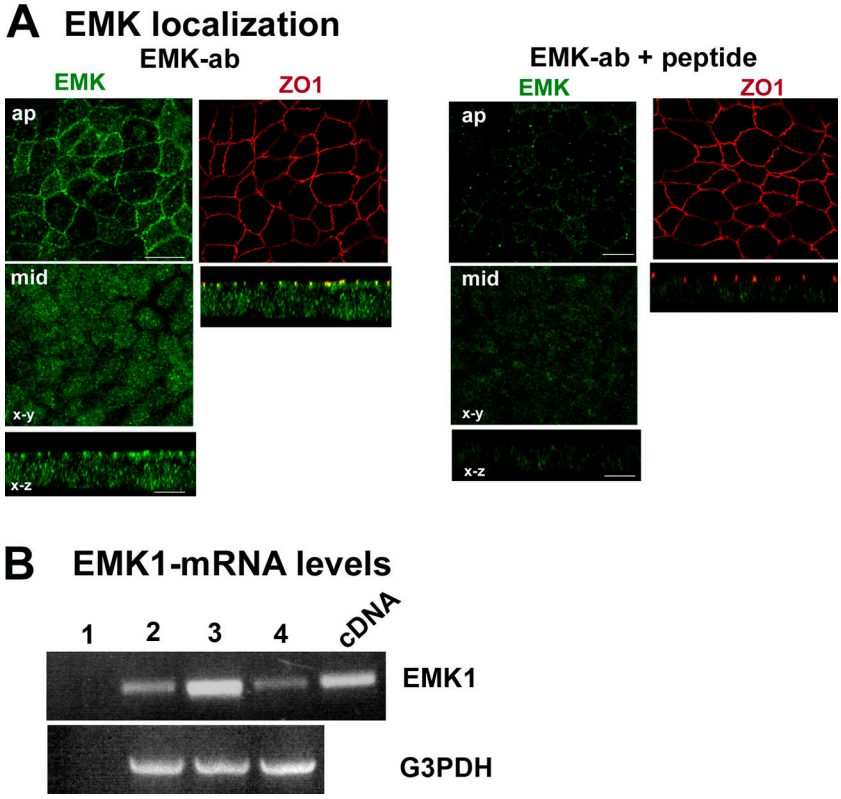

Figure 1. **Endogenous EMK1 in MDCK cells.** (A) EMK localizes at the tight junctions: x-y confocal sections at the tight junction region (ap) and at a mid-plane (mid) and a confocal vertical view (x-z) of MDCK cells labeled for EMK (green) and ZO1 (red) in the absence (left) or presence (right) of the COOH-terminal EMK peptide used as an antigen to raise and purify the antibody. Note that the soluble antigen competes with EMK at tight junctions and reduces intracellular labeling. Bars, 10 μm. (B) EMK1 mRNA levels are regulated during the development of polarity RT-PCR from noncontacting (lane 2), just contacting (lane 3), and 3-d confluent (lane 4) MDCK cultures; (lane 1) control PCR without template. Top, amplification with EMK1 primers; right lane, EMK1 cDNA; bottom, amplification with primers for G3PDH, a housekeeping gene.

at cortical sites have not been elucidated. Polarized hepatic cells also organize their MT noncentrosomally; unlike simple epithelia, the general orientation of these arrays is horizontal, with the negative ends facing an MTOC under the BC (Meads and Schroer, 1995). No mechanisms have been identified that control the MT rearrangements observed in polarizing epithelial cells or the differential MT arrangements observed in simple and hepatic epithelia. Therefore, the relevance of MT reorganization for lumen formation remains unclear.

A clue on which molecules might be controlling the MT organization responsible for polarized apical trafficking and perhaps for polarized lumen formation is provided by studies in organisms especially amenable to genetic analysis. PAR-1 is a serine/threonine kinase that was shown to be essential for the establishment of polarity in the *Caenorhabditis elegans* zygote (Guo and Kemphues, 1995) and the *Drosophila melanogaster* oocyte (Shulman et al., 2000; Tomancak et al., 2000). Its mammalian homologues, the family of EMK/MARK proteins, regulate polarity in neuronal cell models (Biernat et al., 2002) and appear to function redundantly in phosphorylating MT-associated proteins and in regulating MT stability (Drewes et al., 1998). Likewise, evidence in *D. melanogaster* suggests that at least some aspects of PAR-1 function in embryonic polarity involve MT-dependent events (Cox et al., 2001; Vaccari and Ephrussi, 2002). Moreover, recent studies in *D. melanogaster* follicle epithelia have suggested that PAR-1 localizes to the lateral surface and regulates cell shape and monolayer integrity as well as MT stability and organization in this epithelium (Cox et al., 2001; Doerflinger et al., 2003). In contrast, Hurd and Kemphues (2003) found no polarity defects in PAR-1–deficient vulva epithelia of *C. elegans* but reported a role for PAR-1 in cellular process extension and cell–cell contact during vulva morphogenesis. Bohm et al. (1997) have suggested that EMK1/MARK2 regulates polarity in the dog kidney cell line MDCK based on its association with the lateral surface and on the observation that cells expressing dominant-negative EMK1 change shape and lose adhesion to their neighbors. The changes in cell shape and apico-basal polarity elicited by PAR-1 inhibition in different epithelial systems together with the observation that PAR-1 is a kinase for MT-associated proteins make this gene product an excellent candidate to test the hypothesis that the MT cytoskeleton regulates lumen formation in epithelial cells.

In the studies reported here, we have used siRNA to EMK1 and a dominant-negative form of the kinase to knock down its function in two models for columnar epithelial cell (MDCK) polarization, collagen overlay (Hall et al., 1982), and Ca^{2+} switch (Gonzalez-Mariscal et al., 1990) and a model for liver cell polarization (WIFB9; Ihrke et al., 1993). We demonstrate that EMK1/MARK2 is essential for the de novo formation and positioning of luminal domains and for the development of nonradial, epithelial-specific MT arrays in polarizing columnar and hepatic epithelial cells. Our additional experiments show that high expression levels of EMK1 during polarization of MDCK cells promote the appearance of numerous intercellular lumina and a horizontal MT arrangement, both typical of the hepatocyte phenotype, whereas overexpression of the kinase in fully polarized cells only affected MT organization. The data demonstrate an important regulatory role of PAR-1 in the acquisition of epithelial-specific MT arrays that control the generation of polarized lumina in columnar and hepatic epithelia. Further-

more, they support previous findings (Vega-Salas et al., 1987; Ojakian et al., 1997) that indicate that a transient "hepatic" phenotype characterized by the presence of intercellular lumina is an intermediate stage in the de novo generation of polarity by simple columnar epithelia.

Results

EMK inhibition prevents lumen formation and columnar cell shape in MDCK cells

We raised an antibody against the conserved COOH terminus of EMK kinases. As previously shown (Bohm et al., 1997), MDCK cells expressed EMK at the lateral surface (Fig. 1 A). In our hands, most of the membrane-associated protein was concentrated at the level of the apical junctional complex that encompasses tight and adhesion junctions (for review see Mitic and Anderson, 1998), rather than diffusely distributed over the lateral membrane. In addition, the antibody labeled a cytosolic pool of the kinase. MDCK cells drastically increase EMK1 mRNA levels as they undergo polarization and down-regulate the expression of this kinase again upon confluency (Fig. 1 B). Therefore, we tested the effect of EMK1 down-regulation on the development of MDCK cell polarity. To selectively knockdown EMK1, we transiently expressed RNAi-like transcripts under the polymerase III H1 promotor pSUPER (Brummelkamp et al., 2002) using a novel efficient transfection method that delivers cDNA by electroporation directly into the nucleus of suspended cells with gene expression evident 2 h after transfection (unpublished data). Depletion of EMK1 mRNA was detected by RT-PCR (Fig. 2 A, RT-PCR); this resulted in the loss of 60–70% of the protein 24 h after transfection as shown by immunoblot analysis. EMK RNAi depleted the faster migrating band of a double band (Fig. 2 A, IB, asterisk). Immunofluorescence analysis showed reduced EMK at the lateral membrane and a reduced cytoplasmic pool of the protein (Fig. 2 A). We determined by RT-PCR that MDCK cells express an additional PAR-1 homologue (EMK2) that is likely recognized by our antibody (unpublished data). The analysis of EMK protein levels and distribution in EMK1-KO cells indicates that EMK1 accounts for at least 60–70% of the MDCK EMK proteins and is present at the membrane and in the cytosol.

First, we tested the effect of EMK1 knockdown on the development of MDCK cell polarity in collagen matrices where cells form tubules that resemble the organization of native kidney tissue (O'Brien et al., 2002). When MDCK monolayers grown on a planar collagen matrix are overlaid with additional collagen at the apical surface they remove the apical domain and undergo cell rearrangements before they generate polarity de novo around a central lumen (Fig. 2 B, control; Hall et al., 1982; Ojakian and Schwimmer, 1994; Ojakian et al., 2001) that we labeled for the well-characterized luminal marker gp135 (Ojakian and Schwimmer, 1988). Like control cultures, EMK1-KO monolayers lost their apical surface upon collagen overlay; in contrast to control cultures, they failed to form a lumen de novo (Fig. 2 B, EMK1-KO).

To understand how EMK1 may be involved in the formation of the apical surface, we used the Ca^{2+} switch assay (Gonzalez-Mariscal et al., 1990). When cultured at confluency in Ca^{2+}-depleted medium, MDCK cells do not interact with neighboring cells, and hence fail to form a lateral surface domain ("contact naive" cells; Gonzalez-Mariscal et al., 1990). When prevented from polarizing, apical markers accumulate intracellularly in a specialized vacuolar apical compartment (VAC; see Fig. 4 C, control, 0 h; Vega-Salas et al.,

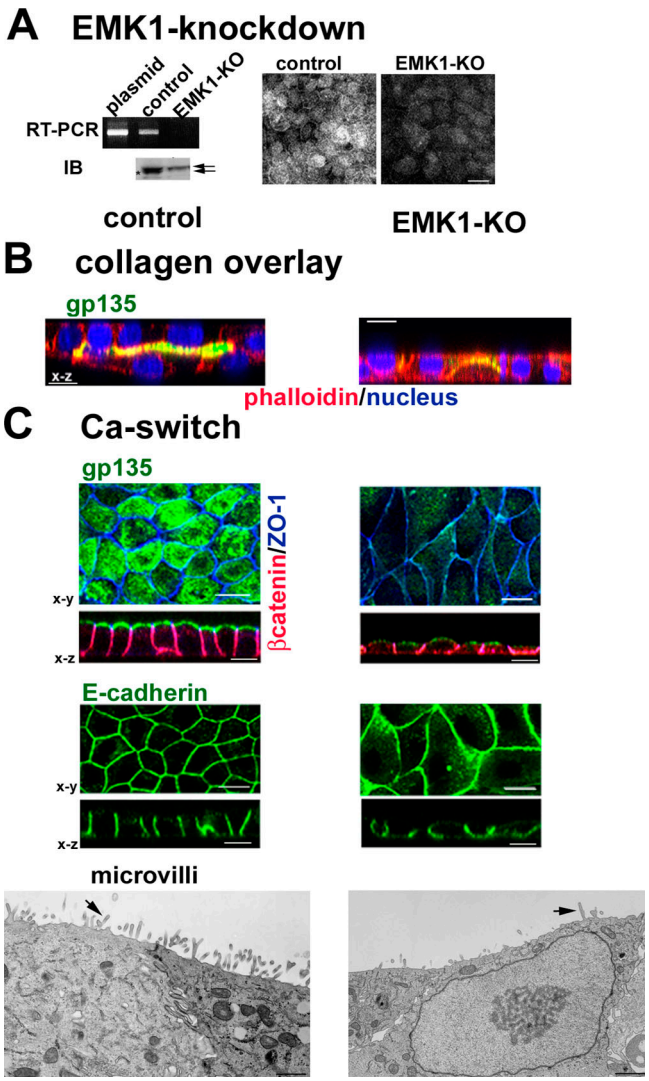

Figure 2. **EMK1 knockdown inhibits lumen formation in MDCK cells.** (A) EMK1 knockdown: left, RT-PCR with EMK1-specific primers of total RNA from control or EMK1-KO cells; EMK1-cDNA was used as a positive control (plasmid); EMK-immunoblot of control and EMK1-KO lysates; asterisk, EMK1 band; right, wide-field image of cells 24 h after transfection with pSUPER (control) or the pSUPER-siEMK1 plasmid (EMK1-KO) taken with the same exposure; cells were immuno-labeled for EMK. (B) Collagen overlay: control (transfected with pSUPER) or EMK1-KO cells were cultured for 24 h on collagen I before being overlaid with additional collagen on the apical surface and analyzed 24 h later. Green, gp135; red, phalloidin; and blue, nucleus. Note the lack of lumen in EMK1-KO cultures. Bars, 10 μm. (C) Ca switch: control or EMK1-KO cells were plated in low Ca medium 24 h upon transfection with pSUPER or pSUPER-KO. After 12 h, cultures were switched to normal medium for 24 h. Top, x-y and x-z confocal projections labeled for gp135 (green), β-catenin (red), and ZO-1 (blue) or for E-cadherin (green). Bars, 10 μm. Bottom, transmission EM of cells sectioned perpendicularly to the substratum; arrow points to microvilli. Bars, 1 μm.

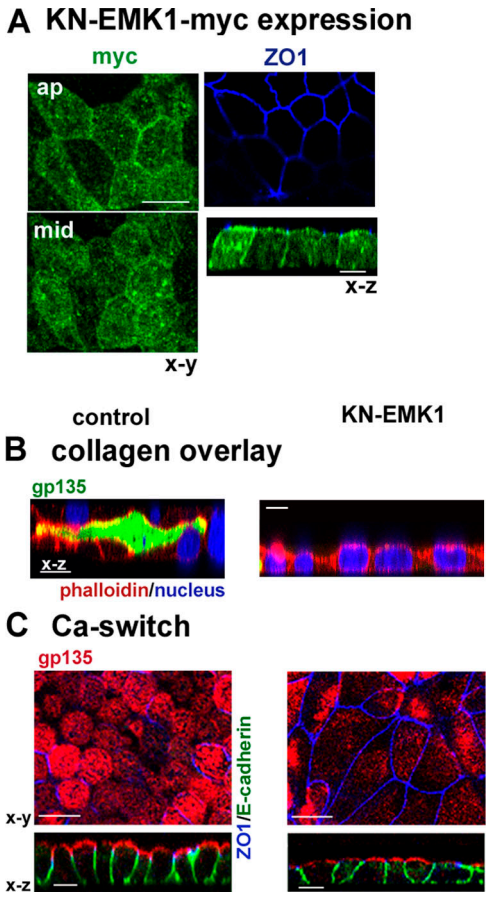

Figure 3. **KN-EMK1 mimics EMK1-KO in MDCK cells.** (A) KN-EMK1-myc expression: x-y confocal sections at the tight junction region (ap) and at a mid-plane (mid) and a confocal vertical view (x-z) of MDCK cells labeled for myc (green) and ZO1 (blue) after expression of myc-tagged KN-EMK1 by adenovirus-mediated gene transfer in fully polarized cells. (B) Collagen overlay: cells were transduced with either control (GFP) or KN-EMK1 virus 12 h after plating on collagen and were cultured for an additional 12 h before collagen overlay for 24 h. x-z view of tubule with gp135 (green) and phalloidin (red); nucleus (blue). Note that KN-EMK1 expression leads to loss of apical domain. (C) Ca switch: contact-naive MDCK cells were transduced with the KN-EMK1 virus or a GFP-virus (control) 12 h before Ca switch for 24 h. Red, gp135; blue, ZO-1; and green, E-cadherin. Bars, 10 μm. Note that intracellular GFP fluorescence is negligible under the virus titer used for infection.

1987). Synchronous cell–cell adhesion induced by addition of normal (1.8 mM) Ca^{2+} levels causes exocytosis of VACs to the cell–cell contact surface. Development of the lateral domain leads to displacement of the lateral lumen to the apex and acquisition of a polarized simple columnar shape.

EMK1 knockdown inhibited the generation of the luminal domain in Ca switch assays. 24 h after Ca switch, when control cells were fully polarized, EMK1-KO monolayers exhibited fivefold less gp135 at the cell surface than control cultures (20 ± 6%; see Materials and methods for details; Fig. 2 C, top). When normalized for the two times larger apical surface area (Fig. 2 C) individual EMK1-KO cells had 40% of surface gp135 of control cells. We obtained similar results for the apical protein GP114 (Fig. S1, top, available at http://www.jcb.org/cgi/content/full/jcb.200308104/DC1; Le Bivic et al., 1990). That EMK1-KO MDCK cells exhibited a defect in apical surface formation was further evidenced by the reduction of the number of microvilli-specific differentiations of the apical domain (Fig. 2 C, microvilli). Pulse–chase analysis revealed that EMK1-KO drastically reduced the half-life of apical proteins at the cell surface (unpublished data). In contrast, basolateral markers such as Na-K-ATPase and the cell–cell adhesion complexes of E-cadherin and β-catenin were present at the lateral domain at comparable levels in control and EMK1-KO cells (Fig. 2 C, bottom panels, and not depicted for Na-K-ATPase). However, EMK1-KO prevented MDCK cells from compacting and fully developing their columnar cell shape. The length of the lateral domain was 6 ± 2 μm in EMK1-KO cells versus 12 ± 3 μm in control. EMK1-KO monolayers reached only 50% of the packing density of control cultures at confluency (Fig. 2 C, x-z). Despite their reduced length, EMK1-KO cells distributed the apical and basolateral proteins remaining at the cell surface into polarized domains separated by tight junctions (Fig. 2 C, Ca switch, x-z). These data indicate that EMK1 is required both for the formation of a mature luminal domain and for the full development of columnar cell shape in polarizing MDCK cells.

We obtained similar results as those described for EMK1 knockdown when we expressed a kinase-deficient form of EMK1, kinase-negative EMK1(KN-EMK1), which has been suggested to act in a dominant-negative fashion (Bohm et al., 1997). We found that recombinant KN-EMK1, expressed by adenovirus-mediated gene transfer in polarized cells (Fig. S2, available at http://www.jcb.org/cgi/content/full/jcb.200308104/DC1), accumulated like the endogenous kinase at the apical junctional complex and showed intracellular labeling; in addition, labeling also extended along the lateral domain (Fig. 3 A). Transduction of MDCK cells with a virus carrying the recombinant protein, but not with a control virus, inhibited tubulogenesis and lumen formation in collagen overlay assays (Fig. 3 B). KN-EMK1 also caused a reduction in gp135 levels at the cell surface and prevented cell compaction and growth of the lateral domain in Ca switch assays resulting in cells with a reduced height (Fig. 3 C). In contrast to the dramatic changes caused by KO or KN-EMK1 expression in polarizing MDCK cells, expression of KN-EMK1 after cells had fully established polarity (i.e., transduction of monolayers after 3 d at confluency) did not affect cell shape and had no obvious effect on the appearance or position of the luminal domain (unpublished data).

EMK1 promotes the appearance of intercellular lumina in MDCK cell cultures

Given the striking effects of EMK1 knockdown on the generation of luminal domains in MDCK cells, we were interested in investigating the effect of increased expression of the kinase on lumen morphogenesis. We performed gain-of-function experiments by inducing 10-fold overexpression of recombinant canine EMK1 protein under a tetracycline-regulated promotor, TET OFF (Fig S2, TET-OFF cells). As with KN-EMK1, the recombinant wild-type protein, when induced in polarized cells, extended from the tight junction region along the lateral domain (Fig. 4 A).

Increased EMK1 expression during polarization of MDCK cells had striking effects on lumen morphogenesis. In col-

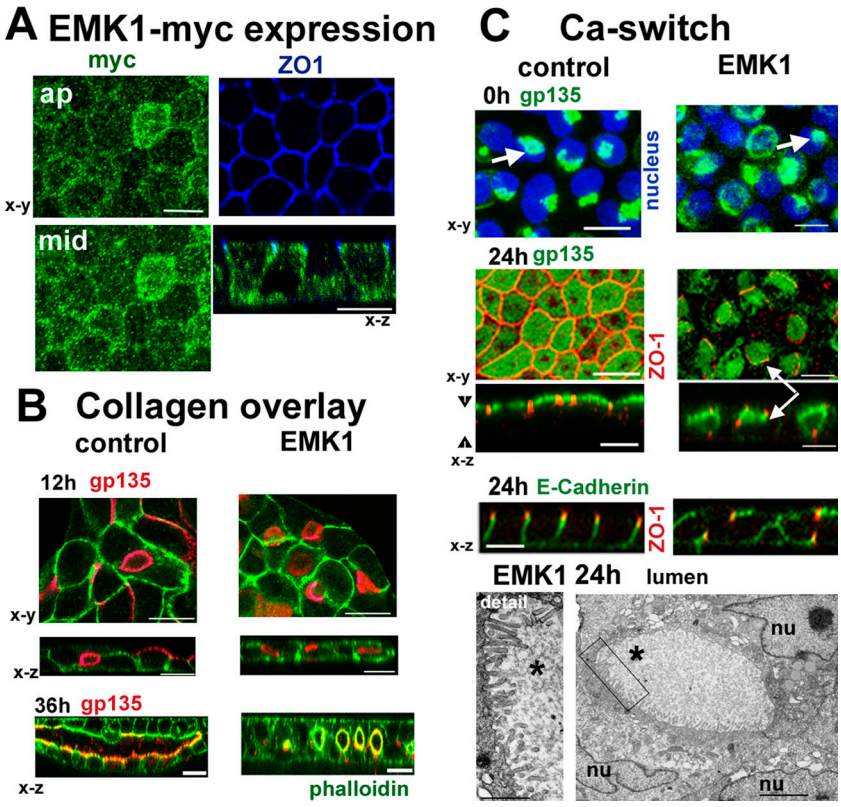

Figure 4. **EMK1 promotes lateral lumina in MDCK cells.** Wild-type EMK1 was expressed in polarized (A) or in polarizing (B and C) MDCK cells under a tetracycline promotor; control, EMK1 + tet; EMK1-overexpressing cells, EMK1 − tet. (A) Recombinant EMK1-myc expression: x-y-confocal sections at the tight junction region (ap) and at a mid-plane (mid) and a confocal vertical view (x-z) of MDCK cells labeled for myc (green) and ZO1 (blue) after expression of myc-tagged wild-type EMK1 by doxycycline withdrawal from fully polarized cells. Bars, 10 μm. (B) Collagen I overlay: subconfluent monolayers were grown on a collagen I substrate and overlaid with collagen I for 12 (top) or 36 h (bottom); confocal x-z sections depicting the lumen between two cell layers; red, gp135; green, FITC-phalloidin. Bars, 10 μm. (C) Ca switch: filter-grown cells 0 or 24 h after Ca switch. (top) Green, gp135; red, ZO-1, and blue, nucleus. x-y and x-z sections; arrows indicate VACs (0 h) and lateral lumina (24 h); arrowheads indicate the positions of the cell apex and cell base. (middle) E-cadherin (green) and ZO-1 (red) 24 h after Ca switch. Bars, 10 μm. (bottom) Transmission EM of EMK1-cells sectioned parallel to the substratum 24 h after Ca switch; three cells ("nu" indicates nucleus) are arranged around a lumen (asterisks); note microvilli in the lumen that is enlarged in the detailed image on left. Bars: (right) 2 μm; (inset) 1 μm.

lagen overlay assays, MDCK cells overexpressing EMK1 formed multiple lateral lumina (Fig. 4 B, 36 h). Similarly, in Ca switch assays, EMK1-MDCK cells established their luminal domain not at the apex but as intercellular lumina between neighboring cells. These lateral lumina were enriched in the apical markers GP135 (Fig. 4 C, 24 h, gp135) and GP114 (Fig. S1, x-z) and featured microvilli characteristic of the apical surface in control cells (Fig. 4 C, transmission EM). The cultures maintained lateral lumina for at least 5 d after Ca switch (unpublished data). Similar intercellular lumina appeared, albeit transiently, in control cultures 12 h after collagen overlay (Fig. 4 B, 12 h; Ojakian et al., 1997) and after exocytosis of VACs toward the lateral membrane upon Ca switch (Vega-Salas et al., 1988; see Fig. 2 D in Cohen and Müsch, 2003). Therefore, our data are consistent with a model in which EMK1 overexpression arrests an intermediate polarity phenotype with lateral lumina, reminiscent of hepatocyte BC during the development of columnar polarity. Expression of KN-EMK1 blocked the effect of EMK1 overexpression on MDCK cells, further establishing the recombinant protein as dominant-negative EMK (Fig. S3, available at http://www.jcb.org/cgi/content/full/jcb.200308104/DC1).

Overexpression of EMK1 after the cells were fully polarized did not cause morphological changes or changes in the position of the luminal domain, indicating that EMK1 promotes hepatic-type lumina only during the development of polarity in MDCK cells. Together with the results from KN-EMK1 expression in fully polarized MDCK cells, these data indicate that the kinase functions in the generation rather than in the maintenance of epithelial luminal domains.

EMK1 regulates BC formation in WIFB9 cells

The gain-of-function experiments demonstrating the generation of hepatocyte-like lumina in MDCK cells prompted us to test whether EMK1 also regulates lumen morphogenesis in the hepatic model cell line WIFB9 (Ihrke et al., 1993). We confirmed published results that showed that WIFB9 cells develop typical hepatocyte polarity over a period of 15 d (Decaens et al., 1996). After 5 d in culture, cells formed monolayers with a polarity similar to that of intestinal or kidney epithelial cells; i.e., the cells expressed the luminal markers dipeptidyl aminopeptidase IV (DPPIV) and HA4 (not depicted) and the tight junction protein ZO1 at their apical poles, and the basolateral markers CE9 and E-cadherin (not depicted) at their basolateral domains (Fig. 5 B, day 5). Subsequently, WIFB9 cells lost their luminal surface (Fig. 5 C, note the absence of DPPIV from many control cells [GFP] at day 9) before they reaccumulated luminal markers in intercellular BC-like lumina characteristic of polarized hepatocytes (Fig. 5 B, day 15).

Like MDCK cells, WIFB cells express EMK1 mRNA (unpublished data) and distribute EMK at the level of their tight junctions and in the cytoplasm (Fig. 5 A, endogenous EMK). The tight junctions of WIFB cells surround the BC-like intercellular lumina formed by the plasma membranes of neighboring cells just as they form a belt limiting the apical domains of columnar epithelia (Fig. 5 A, ZO1 and phase). Because WIFB9 cells are known to be resistant to transient transfection, we studied the role of EMK1 by expressing KN-EMK1 via adenovirus-mediated gene transfer (Fig. S2, KN-EMK1). Transduction with the KN-EMK1 adenovirus for 48 h during the development of WIFB9 polarity at days 5, 7, or 9 inhibited the formation of new translucent vacuoles and

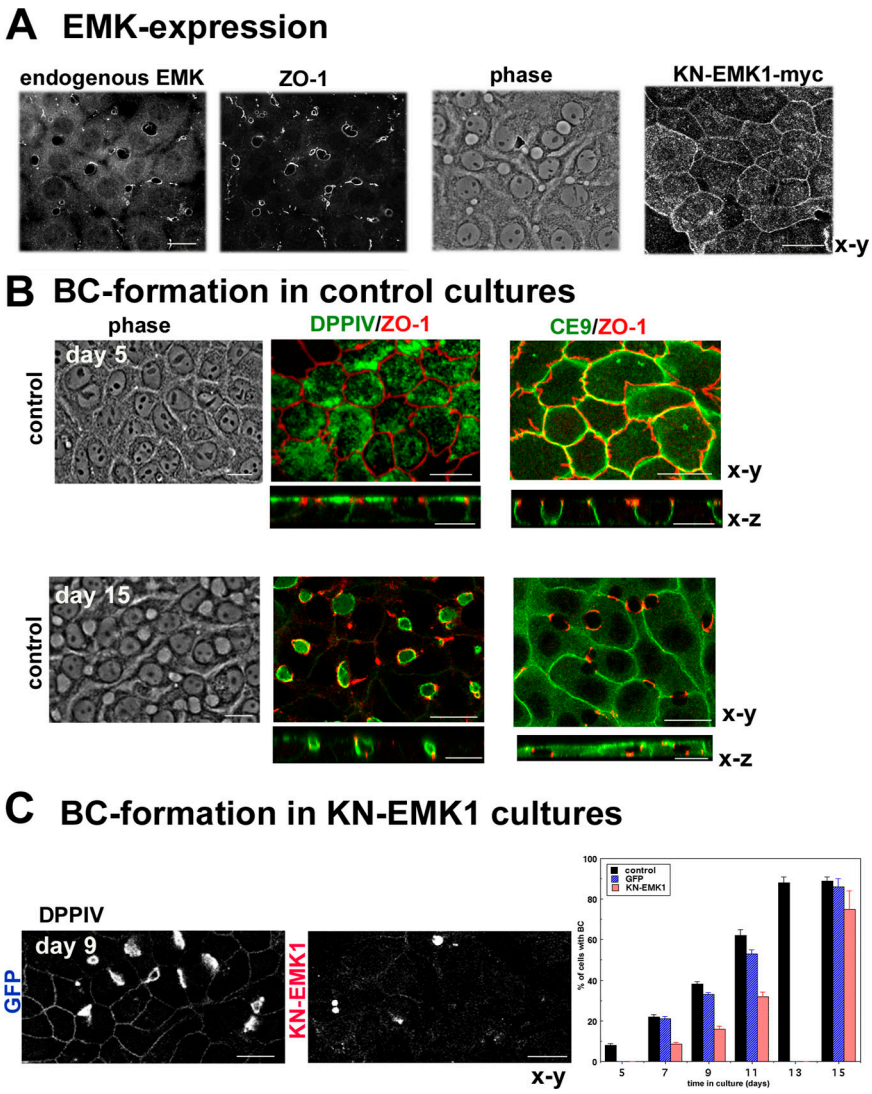

Figure 5. **EMK1 regulates BC formation in WIFB9 cells.** (A) EMK1 localization: (left) x-y wide-field images of cells in phase (right) and colabeled for EMK (left) and ZO-1 (middle); (far right) wide-field image labeled for myc after expression of myc-tagged KN-EMK1 by adenovirus-mediated gene transfer. (B) BC formation in control cells: x-y phase and confocal fluorescence images of cells labeled for DPPIV, CE9 (green), and ZO1 (red) at day 5 (top) or day 15 (bottom) after plating. (C) BC formation upon KN-EMK1 expression cells were transduced with a GFP-control virus (GFP) or with KN-EMK1 expressing adenovirus 48 h before analysis. Bars, 10 μm. (fluorescence) DPPIV in control and KN-EMK1 cells at day 9; (histogram) BCs, identified as intercellular translucent holes, were counted in phase images from ~1,500 cells at day 5, 7, 9, 11, 13, and 15 after plating. Cells were infected at day 5, 7, 9, and 13 with equal pfu of GFP (blue bars) or KN-EMK1 (red bars) expressing adenovirus and analyzed 48 h after infection; black bars, uninfected cells. Data are from three independent experiments. Bars, 10 μm.

BCs when analyzed by phase microscopy (Fig. 5 C, histogram). Cells without translucent lumina had little apical marker when analyzed by immunofluorescence (Fig. 5 C, GFP and KN-EMK1). In contrast, basolateral and tight junction markers remained polarized and organized with columnar polarity (unpublished data). KN-EMK1 had only a very small inhibitory effect on the BC of fully polarized WIFB9 cells (Fig. 5 C, histogram, day 15). The recombinant kinase was far less effective in abolishing previously formed BC than in preventing them from being formed. These data indicate that, as shown for columnar MDCK cells, EMK1 is essential for the generation of a luminal domain in the hepatic epithelial cell line WIFB but is dispensable for the maintenance of this domain.

The effects on lumen morphogenesis are secondary to regulation of MT organization by EMK1

What subcellular system could mediate the effects of PAR-1 on epithelial lumen formation? Because PAR-1 homologues have been identified as MT-regulating kinases in other models (Drewes et al., 1998) and apical protein traffic is MT dependent (for review see Grindstaff et al., 1998), we performed experiments to study EMK1s participation in the organization of MTs in WIFB9 and MDCK cells. In WIFB9 cells, MTs run along a horizontal axis with their negative ends concentrated around the MTOC located immediately next to the BC lumina (Meads and Schroer, 1995; Fig. 6, WIFB9, control). In columnar MDCK cells, the MTOC localizes immediately under the apical surface where the sub-apical MT network is present (Bacallao et al., 1989; Fig. 6, MDCK, control). KN-EMK1 expression in polarizing WIFB9 cells inhibited the development of a hepatocyte-like MT organization, resulting in a radial MT array that originated from a juxtanuclear MTOC, which is characteristic of fibroblastic and nonpolarized epithelial cells (Fig. 6, WIFB9, KN-EMK1). Conversely, EMK1 overexpression in MDCK cells during Ca switch induced a liver-like MT organization, with MTOC and converging MTs adjacent to the lateral lumina (Fig. 6, MDCK, EMK1). These experiments demonstrate that EMK1 induces a liver-like MT organization in MDCK cells.

Is the MT reorganization induced by EMK1 a primary effect of the kinase or is it secondary to its induction of luminal surfaces? To answer this question, we studied the effect of EMK1 overexpression on MT organization in fully polarized MDCK cells where EMK1 did not reorganize the posi-

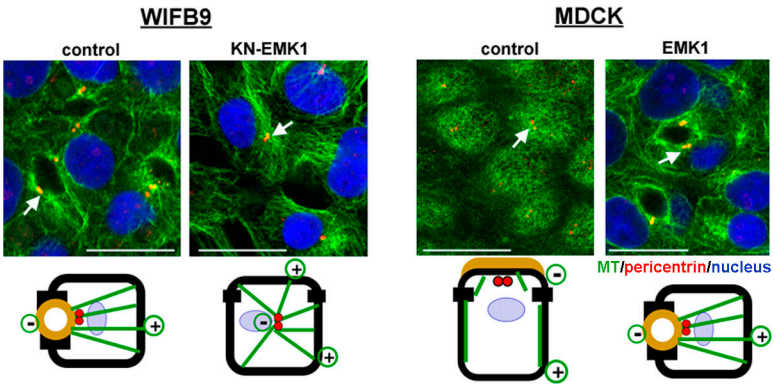

Figure 6. **EMK1 promotes a hepatic MT organization.** WIFB9 cells at day 11, 2 d after expression of a GFP virus (control) or KN-EMK1 adenovirus (KN-EMK1); EMK1-MDCK cells 24 h after Ca switch in the presence (EMK1) or absence (control) of the recombinant kinase. Confocal sections at the plane of the centrosome; pericentrin, a centrosomal marker (red), MT (green), and nucleus (blue). (scheme) Red, centrosome; green, MT with their +/− end orientation; and brown, luminal markers. Arrows indicate centrosomes. Bars, 10 μm. Note that cells were detergent extracted before fixation, leading to complete GFP extraction in WIFB control cells.

tion of the apical domain (unpublished data; discussed in EMKI promotes…cell cultures section). Overexpression of the kinase in polarized MDCK cells significantly reduced the apical MT web while increasing the density of MTs running along the lateral membrane (Fig. 7 A, MT organization, control and EMK1). The reduced apical MT network in EMK1 MDCK cells was highly sensitive to depolymerization by nocodazole, in stark contrast with the apical MT network of control MDCK cells, which was stable in the presence of nocodazole (Fig. 7 A, MT stability, ap). Importantly, the thick lateral MT layer promoted by EMK1 was also sensitive to nocodazole (Fig. 7 A, MT stability, mid), suggesting that it did not result from long-term stabilization of MT but, rather, from increased assembly of MT at the lateral cortex. EMK1 overexpression in polarized MDCK cells also displaced the MTOC toward the lateral surface (Fig. 7 A, MT nucleation). MTOC displacement might contribute to increased MT assembly at the lateral cortex and to the reduced apical web. Alternatively, changes in MT organization might be the cause for the displacement of the MTOC, as a similar MTOC displacement had been observed in cells with disrupted apical MT organization in the intestinal cell line Caco2 (Salas et al., 1997; Balczon et al., 1999).

Additional evidence for EMK1's primary role as inducer of lateral MT assembly in MDCK cells was provided by EMK1-KO. This treatment caused a drastic reduction in vertical MT (Fig. 7 A, MT organization, EMK1-KO). The juxtanuclear localization of the MTOC and the absence of a nocodazole-resistant apical MT web further suggests that EMK1 knockdown cells fail to establish an epithelial-specific MT network (Fig. 7 A, MT stability and MT nucle-

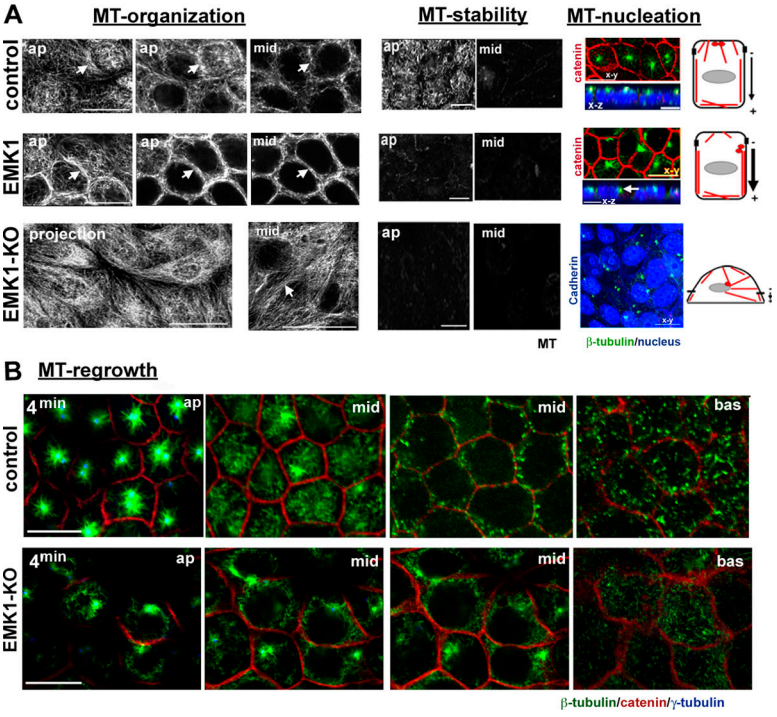

Figure 7. **EMK1 promotes MT assembly at the lateral cortex in MDCK cells.** (A) Recombinant EMK1 was induced by doxycycline withdrawal from EMK1-MDCK cells after they had polarized (EMK1); endogenous EMK1 was knocked down (EMK1-KO) by transfection with an EMK1-siRNA vector, and cells were cultured for 48h; controls shown are representative of EMK1-MDCK cells maintained in doxyxycline and of MDCK cells transfected with control siRNA-vector. MT organization, confocal sections of MT at the most apical (ap) and at mid-plane (mid); arrow, MT at lateral cortex; MT stability, apical and lateral MT after 1 h nocodazole treatment at 37°C; and MT nucleation, MT asters (green) that represent the MT nucleation center during MT repolymerization after cold treatment. β-tubulin labeling is in green in all panels. In addition, control and EMK1 cells show β-catenin (red) in the x-y views or the nucleus (blue) in x-z-views. Pericentrin, a centrosomal marker (red), localizes to the β-tubulin aster in the x-z sections. In EMK1-KO cells, E-cadherin and the nucleus are labeled in blue. Bars, 10 μm. Models (right): schematic depiction of the differences in centrosome localization (red dots) and MT arrangements (red lines); black arrows indicate amount of vertical MTs. (B) MT regrowth: serial apical to basal x-y sections from control and EMK1-KO cells labeled for MTs (green), β-catenin (red), and γ-tubulin (blue) 4 min after nocodazole washout. Note MTs released from the MTOC (labeled by γ-tubulin; asterisks) at the lateral cortex in control cells and in the perinuclear region in EMK1-KO cells (arrows). Bars, 10 μm.

ation, EMK1-KO), similar to the situation in WIFB9 cells upon expression of dominant-negative EMK1. We established in MT regrowth experiments after nocodazole washout that EMK1-KO does not prevent the release of newly nucleated MTs from the MTOC but rather their capture at cortical sites (Fig. 7 B). In summary, our data suggest that EMK1 stimulates assembly of MT at the cell cortex and is required for the conversion of the radial MT array of nonpolarized epithelia into a MT network organized along the apico-basolateral polarity axis of polarized epithelial cells.

Discussion

Formation of epithelial lumina is regulated by EMK1

Using two models of columnar epithelial cell polarization and one model of hepatocyte polarization (Fig. 8) we have shown that de novo formation of luminal domains requires endogenous expression of EMK1, a kinase of MT-associated proteins. In the first model, MDCK cells kept in low Ca medium stored luminal markers intracellularly that underwent exocytosis toward the sites of cell–cell contact on switch to normal Ca levels (Fig. 8, top path). EMK1-KO or KN-EMK1 expression before and during Ca switch EMK1 drastically reduced the amount of apical markers that appeared at the cell surface. In the second model, collagen overlay of MDCK cells (Fig. 8, middle path), columnar epithelial polarity breaks down upon addition of a collagen gel, and luminal markers become transiently undetectable; they reappear to form first intercellular lateral lumen and eventually a new central lumen. EMK1-KO or KN-EMK1 inhibited cell rearrangements and lumen formation in this tubulogenesis model. In the third model, cultures of the hepatocyte cell line WIFB9 (Fig. 8, bottom path) develop lateral lumina with characteristics of BC through intermediate stages of acquisition and loss of columnar polarity (Decaens et al., 1996, Tuma et al., 2002). In this model, dominant-negative EMK1 inhibited formation of BC-like lateral lumina. All of these results suggest that EMK1 is necessary for the early steps of lumen morphogenesis in both columnar and hepatic epithelia.

Additional experiments with the same model systems further indicated that EMK1 also participates in the determination of the final position of the luminal domain. EMK1 overexpression in MDCK cells induced lateral lumina reminiscent of the BC in hepatocytes. Transient intercellular lumina have been demonstrated during MDCK polarization in both the collagen overlay and the Ca switch models (Vega-Salas et al., 1987; Ojakian et al., 1997). These transient intercellular lumina are most likely a real feature of epithelial development and not merely a tissue culture artifact as they have been observed in developing and transformed epithelia (for review see Vega-Salas et al., 1988). Our data support a scenario in which EMK1 signaling not only regulates the acquisition of a luminal domain by epithelial cells (Fig. 8, 1) but also the developmental branching decision between a columnar and a hepatocyte polarity phenotype (Fig. 8, 2). In this scenario, lower EMK1-signaling levels promote progression via a lateral lumen intermediate toward a columnar phenotype, whereas higher EMK1-signaling levels arrest cells at the intercellular lumen stage. In apparent agreement with this model, MDCK cells that were starting to undergo polarization displayed the highest EMK1 mRNA levels; in contrast, nonpolarized and fully polarized MDCK cells expressed lower levels of EMK1 (Fig. 1 B). However, the EMK1-signaling levels may not be directly related to its mRNA levels. Our model predicts that polarized hepatocytes maintain higher EMK1-signaling levels than columnar epithelia. However, a meaningful comparison will require the elucidation of the EMK1-signaling cascade.

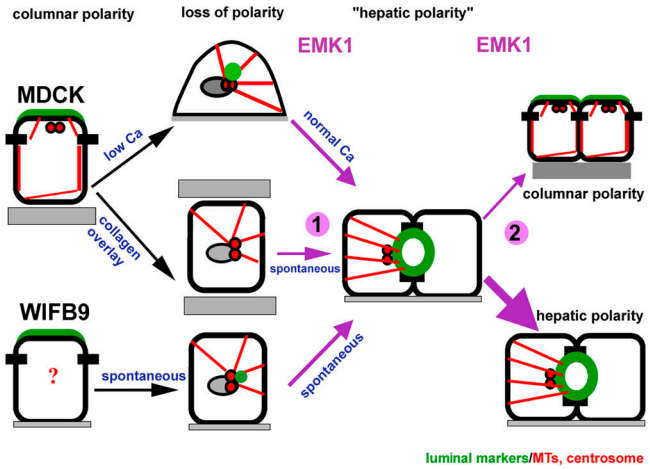

Figure 8. **EMK1 regulates MT and lumen polarity in a two-step process.** The three model systems used in this work: Ca switch in MDCK cells (top path), collagen overlay of MDCK monolayers (middle path), and long-term cultures of the hepatocyte cell line WIFB9 (bottom path). In all systems, columnar polarity is lost transiently, either upon culture in low Ca^{2+} levels or addition of collagen overlay (MDCK), or by spontaneous loss of a transitional columnar stage (WIFB9). In the nonpolarized state, luminal markers (green) accumulate in intracellular storage compartments (MDCK before Ca switch; WIFB) or are undetectable (MDCK cells under collagen overlay) and the MTs (red lines) have a radial arrangement (MTOC, red dots). Increased EMK1 signaling (1) causes conversion of the nonpolarized stage into a "hepatic polarity stage" with a horizontal MT array and a subluminal centrosome and luminal domains at sites of cell–cell contact (VAC exocytosis in Ca switch, spontaneous intercellular lumen formation in collagen overlay and in WIFB9 cells). In step 2, EMK1-signaling levels regulate the final polarity of the epithelium. High EMK1-signaling levels, as in EMK1-overexpressing MDCK cells or in WIFB9 cells (hypothetical in this case), consolidate lateral lumen polarity and horizontal MT organization ("hepatic-type"). Lower EMK1-signaling levels, such as in control MDCK cells, lead to a relocalization of the luminal domain to the cell apex and vertical MT (columnar organization).

The use of a dominant-negative kinase and acute protein knockdown in cell culture systems allowed us to discover a role for EMK1 in epithelial morphogenesis that was not apparent in EMK1 knockout mice (Bessone et al., 1999; Hurov et al., 2001). The lack of gross morphogenetic defects in EMK1-KO mice is most likely due to compensation by one of three other EMK kinases that are ubiquitous and act redundantly when expressed in different experimental systems (Ebneth et al., 1999, Sun et al., 2001). As in the case of the caveolin knockout mouse, compensatory mechanisms that work in the context of the entire organism do not always operate in the context of cell culture models (for review see Razani and Lisanti, 2001).

The acquisition of an apico-basolateral MT array during epithelial polarization is regulated by EMK1

In parallel with the effects on lumen formation, inhibition of EMK1 expression also affected MT reorganization associated with epithelial polarization. Inhibition of EMK1 expression at the time when polarity was being established prevented the development of a vertical polarized MT network in MDCK cells (Fig. 7) and of horizontal MTs in WIFB9 cells (Fig. 6). Under these conditions, MDCK and WIFB9 cells exhibited a radial MT array that emanated from the perinuclear region. In contrast, inhibition of EMK1 function in fully polarized MDCK or WIFB9 cells was not sufficient to reverse either MT or lumen organization, suggesting that EMK1 provides an early cue for the acquisition of both epithelial features but is dispensable for their maintenance.

However, overexpression of EMK1 in MDCK cells undergoing polarization promoted both a hepatic lumen polarity and a hepatic MT organization. As with EMK1 inhibition, overexpression of the kinase in fully polarized MDCK cells did not affect lumen polarity. However, the recombinant kinase induced vertical MTs and reduced the apical MT web in fully polarized cells (Fig. 7). These experiments suggest that the primary function of EMK1 is to promote the organization of epithelial-specific MT arrays, which, in turn, induces alterations in the intracellular transport of luminal proteins. In support of this interpretation, we observed alterations in the trafficking mode for apical proteins elicited by EMK1 expression in fully polarized MDCK cells even though their steady-state distribution was unchanged (unpublished data).

Our data demonstrate that epithelial cells undergoing polarization are susceptible to changes in MT distribution regulated by EMK1 that lead to changes in apical protein trafficking and lumen position. In contrast, fully polarized epithelial cells can change their MT distribution and partially modify their apical protein trafficking under the influence of EMK1, but this is not sufficient to alter the position of their lumina.

A model on the regulation of epithelial lumen morphogenesis by EMK1 localized at the apical junctional complex

Endogenous EMK is polarized to the lateral domain (Bohm et al., 1997) and in our hands enriched at the apical junctional complex. Formation of E-cadherin–mediated adhesions provides the cue to generate identity of the lateral domain in MDCK cells (for review see Yeaman et al., 1999). Forced induction of cell–cell adhesion in centrosome-free cytoplasts obtained from fibroblasts transfected with E-cadherin promotes changes in MT behavior from treadmilling to dynamic instability, which is compatible with stabilization of MT minus ends (Chausovsky et al., 2000). We speculate that newly formed E-cadherin–mediated contacts between neighboring epithelial cells undergoing polarization could activate signaling by membrane-bound EMK1 leading to the capture of MT negative ends, resulting in the establishment of a noncentrosomal MT distribution. In turn, this may lead to a lateral shift in the centrosome localization (also promoted by EMK1; Fig. 7), further reinforcing the noncentrosomal MT distribution. Once negative MT ends are captured at cortical sites, minus end–directed MT motors that mediate apical exocytosis (for review see Noda et al., 2001) could transport intracellular vesicles carrying apical markers (e.g., VACs in the Ca switch model) toward the sites of cell–cell contact. Our data are consistent with a scenario in which moderate EMK1-signaling levels regulate the growth of the lateral membrane and compaction in polarizing MDCK cells and the relocalization of the "luminal targeting patch," required for the fusion of apical transport vesicles, to the developing apical domain. This process likely involves the capture of MT negative ends by a maturing apical cortical cytoskeleton (Salas et al., 1997, Mogensen et al. 2000) and the relocalization of the MTOC beneath the luminal domain. Indeed, recent results indicate that during polarization of MDCK cells, syntaxin 3 changes from a nonpolar distribution to an apical distribution in a process dependent on MT (Kreitzer et al., 2003). According to the same scenario, higher EMK1-signaling levels prevent the relocalization of the luminal targeting patch to the apical membrane by arresting the transient MT organization at the lateral membrane. Elucidation of the EMK1-signaling cascade, currently a main objective in our laboratory, is essential to experimentally test the details of this model.

Materials and methods

Cell culture and virus transduction

Stable cell lines expressing COOH-terminal myc-tagged canine EMK1 in pTRE2 were generated in MDCK-TET-OFF cells (provided by K. Mostov, University of California, San Francisco, San Francisco, CA) that repress the expression of the recombinant protein in the presence of 20 ng/ml of the tetracycline derivative doxycycline. Maintenance of EMK1-MDCK cells was performed as described previously (Cohen et al., 2001). For Ca switch experiments, cells cultured for 24 h in the absence of doxycycline or after transfection with the pSUPER-based cDNA were plated at confluency in S-MEM (Sigma-Aldrich) with 10% FCS dialyzed against PBS and maintained for 12 h before the switch to normal growth medium. Collagen I overlay of subconfluent monolayers grown on collagen-coated coverslips was done as described previously (Hall et al., 1982). WIFB9 cells (provided by A. Hubbard [Johns Hopkins University, Baltimore, MD] and D. Cassio [Univerisite Paris-Sud, Orsay, France]) were cultured as described previously (Shanks et al., 1994). Adenovirus infection was in Opti-MEM for 2 h with four plaque-forming units (pfu)/cell. Virus titers were determined by plaque assays according to Falck-Pedersen (1998). All viruses were adjusted to the same measurement (pfu/ml). Cells were analyzed 48 h after adenovirus transduction.

cDNA generation and expression

Canine EMK1 was cloned from an MDCK ZAPII library (provided by M. Zerial, Max Planck Institute for Molecular Cell Biology and Genetics, Dresden, Germany) and shows 99.3% similarity with the short splice variant of human EMK1 (GenBank/EMBL/DDBJ accession no. NM 004954). The NH_2-terminal 810 bp encoding the kinase domain were deleted in the KN-EMK1 cDNA. Recombinant adenoviruses expressing GFP (the nonenhanced version) or KN-EMK1-myc were generated and propagated as described previously (Cohen et al., 2001). For RT-PCR, 2 μg of total RNA was reverse transcribed with oligo-dT primers; 1 μl of the first strand reaction was amplified with either rat G3PDH primers (Promega) or with EMK1 (primers: 5′caggtgcgggaccagcaga3′; 5′tggctattttggaggcaatgtt3′) that completely match the canine, rat, and human sequences. Knockdown of EMK1 by siRNA was performed by cloning the annealed sequences 5′gatccccGAGGTAGCTGTGAAGATCAttcaagagaTGATCTTCACAGCTACCTCtttttggaaa3′ and 5′agcttttccaaaaaGAGGTAGCTGTGAAGATCAtctcttgaaTGATCTTCACAGCTACCTCggg3′ into the vector pSUPER (Brummelkamp et al., 2002; provided by R. Agami, The Netherlands Cancer Institute, Amsterdam, Netherlands). Transient transfection of the RNAi plasmid was performed by nucleofection with Amaxa™ technology using 20 μg of cDNA/4 × 10^6 cells. Cells were analyzed 48 h after transfection.

Antibodies

A rabbit polyclonal EMK/MARK antibody was raised against a GST-fusion protein with the COOH-terminal 310 aa of mouse EMK2 (EST I.M.A.G.E. clone; GenBank/EMBL/DDBJ accession no. aa162350) that was conserved among MARK family members and affinity purified.

Other antibodies used were as follows: myc, clone 9E10 (Santa Cruz Biotechnology, Inc.); gp135 (clone 3F21D8; provided by G. Ojakian, SUNY Downstate Medical Center, Brooklyn, NY), gp114 (Balcarova-Stander et al., 1984), rat monoclonal ZO-1 (Chemicon), E-cadherin (BD Biosciences), β-tubulin (clone TUB 2.1; Sigma-Aldrich); γ-tubulin (clone GTU-88; Sigma-Aldrich), pericentrin (Covenance), DPPIV (Serotec), and anti-HA4c19 (Hubbard et al., 1985).

Immunolabeling techniques/quantification

For immunofluorescence, MDCK cells were fixed at RT or on ice (for EMK labeling) with 2% PFA; WIFB9 cells were fixed on ice with 3% PFA; and permeabilization was performed with 0.075% saponin. For MT labeling, cells were extracted for 30 s at 37°C with PEM (100 mM Pipes, pH 6.8, 1 mM EGTA, and 1 mM Mg_2Cl_2) + 0.5% Triton X-100 and fixed in ice-cold methanol. For MT regrowth experiments, cells were kept on ice for 1 h and extracted for 30 s at RT. Confocal microscopy was performed with a model TCS SP2 (Leica) using a 63× oil objective. Presented are individual confocal x-y sections, vertical views, or where indicated x-y-z projections generated with LCS software (Leica). Images were processed with Adobe Photoshop. Phase and wide-field images were acquired with either a 60× oil lens or a 40 or 20× dry objective on a microscope (model E-600; Nikon) equipped with a back-illuminated cooled CCD camera (model 1000-PB; Roper Scientific) and processed with Metamorph software (Universal Imaging Corp.).

Gp135-surface fluorescence was quantified with Metamorph software from 20×-wide field images taken of 10 random fields at the same exposure. To normalize for cell number per surface area, cells in 10 random fields of equal surface area (corresponding to ~100 cells in control monolayers) were counted. Similarly, cell compaction was assessed by determination of the cell number per surface area from 20× phase images taken 24 and 48 h after plating control and EMK1-KO cells at confluency (0.6×10^6 cells/cm^2). Height of the lateral domain was determined with confocal software (Leica) from x-z sections of 10 images taken with a 63× oil lens; data are from two different experiments.

For transmission EM, cells were fixed in 2% glutaraldehyde/PBS + Ca^{2+}/Mg^{2+}, washed with 0.1M Cacodylate, pH 7.4, postfixed in 1% OsO_4, contrasted with 1% aqueous uranyl-acetate, dehydrated, and embedded in Epon-Araldite. Sections were cut perpendicular (Fig. 2) or parallel (Fig. 4) to the filter surface and analyzed in a electron microscope (model 100EX II; JOEL USA, Inc.).

Immunoblots were probed with ^{125}I-protein A and analyzed by phosphorimager (Molecular Dynamics).

Online supplemental material

Fig. S1, Gp114 upon EMK1-KO and EMK1 overexpression in Ca switch assays; Fig. S2, recombinant EMK1 in MDCK and WIFB9 cells; and Fig. S3, KN-EMK1 inhibits lateral lumina in EMK1-MDCK cells. Online supplemental material is available at http://www.jcb.org/cgi/content/full/jcb.200308104/DC1.

We gratefully acknowledge Leona Cohen-Gould for the EM work. We thank Drs. M. Zerial, R. Agami, and G. Ojakian for reagents; D. Cassio and A. Hubbard for the WIFB9 cells; D. Cassio and L. Braiterman for advice in WIFB-cell culture; E. Falck-Pedersen for help with the adenovirus plaque assays; and D. Herzlinger, T. McGraw, G. Gundersen, A. Gonzales, and A. Caceres for helpful discussions.

This work was supported by a Stein Professorship of the Research to Prevent Blindness Foundation (to E. Rodriguez-Boulan), grants GM-34107 (to E. Rodriguez-Boulan) and GM-54712 (to P.J. Brennwald) from the National Institutes of Health, and SDG 0235130N of the American Heart Association (to A. Müsch).

Submitted: 19 August 2003
Accepted: 31 December 2003

References

Achler, C., D. Filmer, C. Merte, and D. Drenckhahn. 1989. Role of microtubules in polarized delivery of apical membrane proteins to the brush border of the intestinal epithelium. *J. Cell Biol.* 109:179–189.

Bacallao, R., C. Antony, C. Dotti, E. Karsenti, E.H. Stelzer, and K. Simons. 1989. The subcellular organization of Madin-Darby canine kidney cells during the formation of a polarized epithelium. *J. Cell Biol.* 109:2817–2832.

Balcarova-Stander, J., S.E. Pfeiffer, S.D. Fuller, and K. Simons. 1984. Development of cell surface polarity in the epithelial Madin-Darby canine kidney (MDCK) cell line. *EMBO J.* 3:2687–2694.

Balczon, R., C.E. Varden, and T.A. Schroer. 1999. Role for microtubules in centrosome doubling in Chinese hamster ovary cells. *Cell Motil. Cytoskeleton.* 42:60–72.

Bessone, S., F. Vidal, Y. Le Bouc, J. Epelbaum, M.T. Bluet-Pajot, and M. Darmon. 1999. EMK protein kinase-null mice: dwarfism and hypofertility associated with alterations in the somatotrope and prolactin pathways. *Dev. Biol.* 214:87–101.

Biernat, J., Y.Z. Wu, T. Timm, Q. Zheng-Fischhofer, E. Mandelkow, L. Meijer, and E.M. Mandelkow. 2002. Protein kinase MARK/PAR-1 is required for neurite outgrowth and establishment of neuronal polarity. *Mol. Biol. Cell.* 13:4013–4028.

Bohm, H., V. Brinkmann, M. Drab, A. Henske, and T.V. Kurzchalia. 1997. Mammalian homologues of *C. elegans* PAR-1 are asymmetrically localized in epithelial cells and may influence their polarity. *Curr. Biol.* 7:603–606.

Bre, M.H., R. Pepperkok, A.M. Hill, N. Levilliers, W. Ansorge, E.H. Stelzer, and E. Karsenti. 1990. Regulation of microtubule dynamics and nucleation during polarization in MDCK II cells. *J. Cell Biol.* 111:3013–3021.

Brummelkamp, T.R., R. Bernards, and R. Agami. 2002. A system for stable expression of short interfering RNAs in mammalian cells. *Science.* 296:550–553.

Chausovsky, A., A.D. Bershadsky, and G.G. Borisy. 2000. Cadherin-mediated regulation of microtubule dynamics. *Nat. Cell Biol.* 2:797–804.

Cohen, D., and A. Müsch. 2003. Apical surface formation in MDCK cells: regulation by the serine/threonine kinase EMK1. *Methods.* 30:269–276.

Cohen, D., A. Müsch, and E. Rodriguez-Boulan. 2001. Selective control of basolateral membrane protein polarity by cdc42. *Traffic.* 2:556–564.

Cox, D.N., B. Lu, T.Q. Sun, L.T. Williams, and Y.N. Jan. 2001. *Drosophila* par-1 is required for oocyte differentiation and microtubule organization. *Curr. Biol.* 11:75–87.

Decaens, C., P. Rodriguez, C. Bouchaud, and D. Cassio. 1996. Establishment of hepatic cell polarity in the rat hepatoma-human fibroblast hybrid WIF-B9. A biphasic phenomenon going from a simple epithelial polarized phenotype to an hepatic polarized one. *J. Cell Sci.* 109:1623–1635.

Doerflinger, H., R. Benton, J.M. Shulman, and D.S. Johnston. 2003. The role of PAR-1 in regulating the polarised microtubule cytoskeleton in the *Drosophila* follicular epithelium. *Development.* 130:3965–3975.

Drewes, G., A. Ebneth, and E.M. Mandelkow. 1998. MAPs, MARKs and microtubule dynamics. *Trends Biochem. Sci.* 23:307–311.

Ebneth, A., G. Drewes, and E. Mandelkow. 1999. Phosphorylation of MAP2c and MAP4 by MARK kinases leads to the destabilization of microtubules in cells. *Cell Motil. Cytoskeleton.* 44:209–224.

Falck-Pedersen, E. 1998. Use and application of adenovirus expression vectors. *In* Light Microscopy and Cell Structure. Vol. 2 of Cells: A Laboratory Handbook. D. Spector, editor. Cold Spring Harbor Laboratory Press, Cold Spring Harbor, NY. 1–28.

Gilbert, T., A. Le Bivic, A. Quaroni, and E. Rodriguez-Boulan. 1991. Microtubular organization and its involvement in the biogenetic pathways of plasma membrane proteins in Caco-2 intestinal epithelial cells. *J. Cell Biol.* 113: 275–288.

Gonzalez-Mariscal, L., R.G. Contreras, J.J. Bolivar, A. Ponce, B. Chavez De Ramirez, and M. Cereijido. 1990. Role of calcium in tight junction formation between epithelial cells. *Am. J. Physiol.* 259:C978–C986.

Grindstaff, K.K., R.L. Bacallao, and W.J. Nelson. 1998. Apiconuclear organization of microtubules does not specify protein delivery from the trans-Golgi network to different membrane domains in polarized epithelial cells. *Mol. Biol. Cell.* 9:685–699.

Guo, S., and K.J. Kemphues. 1995. par-1, a gene required for establishing polarity in *C. elegans* embryos, encodes a putative Ser/Thr kinase that is asymmetrically distributed. *Cell.* 81:611–620.

Hall, H.G., D.A. Farson, and M.J. Bissell. 1982. Lumen formation by epithelial cell lines in response to collagen overlay: a morphogenetic model in culture. *Proc. Natl. Acad. Sci. USA.* 79:4672–4676.

Hubbard, A.L., J.R. Bartles, and L.T. Braiterman. 1985. Identification of rat hepatocyte plasma membrane proteins using monoclonal antibodies. *J. Cell Biol.* 100:1115–1125.

Hogan, B.L., and P.A. Kolodziej. 2002. Organogenesis: molecular mechanisms of tubulogenesis. *Nat. Rev. Genet.* 3:513–523.

Hurd, D.D., and K.J. Kemphues. 2003. PAR-1 is required for morphogenesis of

the *Caenorhabditis elegans* vulva. *Dev. Biol.* 253:54–65.

Hurov, J.B., T.S. Stappenbeck, C.M. Zmasek, L.S. White, S.H. Ranganath, J.H. Russell, A.C. Chan, K.M. Murphy, and H. Piwnica-Worms. 2001. Immune system dysfunction and autoimmune disease in mice lacking Emk (Par-1) protein kinase. *Mol. Cell. Biol.* 21:3206–3219.

Ihrke, G., E.B. Neufeld, T. Meads, M.R. Shanks, D. Cassio, M. Laurent, T.A. Schroer, R.E. Pagano, and A.L. Hubbard. 1993. WIF-B cells: an in vitro model for studies of hepatocyte polarity. *J. Cell Biol.* 123:1761–1775.

Kreitzer, G., J. Schmoranzer, S.H. Low, X. Li, Y. Gan, T. Weimbs, S.M. Simon, and E. Rodriguez-Boulan. 2003. Three-dimensional analysis of post-Golgi carrier exocytosis in epithelial cells. *Nat. Cell Biol.* 5:126–136.

Le Bivic, A., Y. Sambuy, K. Mostov, and E. Rodriguez-Boulan. 1990. Vectorial targeting of an endogenous apical membrane sialoglycoprotein and uvomorulin in MDCK cells. *J. Cell Biol.* 110:1533–1539.

Mays, R.W., K.A. Beck, and W.J. Nelson. 1994. Organization and function of the cytoskeleton in polarized epithelial cells: a component of the protein sorting machinery. *Curr. Opin. Cell Biol.* 6:16–24.

Meads, T., and T.A. Schroer. 1995. Polarity and nucleation of microtubules in polarized epithelial cells. *Cell Motil. Cytoskeleton.* 32:273–288.

Mitic, L.L., and J.M. Anderson. 1998. Molecular architecture of tight junctions. *Annu. Rev. Physiol.* 60:121–142.

Mogensen, M.M., A. Malik, M. Piel, V. Bouckson-Castaing, and M. Bornens. 2000. Microtubule minus-end anchorage at centrosomal and non-centrosomal sites: the role of ninein. *J. Cell Sci.* 113:3013–3023.

Noda, Y., Y. Okada, N. Saito, M. Setou, Y. Xu, Z. Zhang, and N. Hirokawa. 2001. KIFC3, a microtubule minus end–directed motor for the apical transport of annexin XIIIb–associated Triton-insoluble membranes. *J. Cell Biol.* 155:77–88.

O'Brien, L.E., M.M. Zegers, and K.E. Mostov. 2002. Opinion: Building epithelial architecture: insights from three-dimensional culture models. *Nat. Rev. Mol. Cell Biol.* 3:531–537.

Ojakian, G.K., and R. Schwimmer. 1988. The polarized distribution of an apical cell surface glycoprotein is maintained by interactions with the cytoskeleton of Madin-Darby canine kidney cells. *J. Cell Biol.* 107:2377–2387.

Ojakian, G.K., and R. Schwimmer. 1994. Regulation of epithelial cell surface polarity reversal by beta 1 integrins. *J. Cell Sci.* 107:561–576.

Ojakian, G.K., W.J. Nelson, and K.A. Beck. 1997. Mechanisms for de novo biogenesis of an apical membrane compartment in groups of simple epithelial cells surrounded by extracellular matrix. *J. Cell Sci.* 110:2781–2794.

Ojakian, G.K., D.R. Ratcliffe, and R. Schwimmer. 2001. Integrin regulation of cell-cell adhesion during epithelial tubule formation. *J. Cell Sci.* 114:941–952.

Razani, B., and M. Lisanti. 2001. Caveolin-deficient mice: insights into caveolar function human disease. *J. Clin. Invest.* 108:1553–1561.

Salas, P.J., M.L. Rodriguez, A.L. Viciana, D.E. Vega-Salas, and H.P. Hauri. 1997. The apical submembrane cytoskeleton participates in the organization of the apical pole in epithelial cells. *J. Cell Biol.* 137:359–375.

Shanks, M.S., D. Cassio, O. Leqoc, and A.L. Hubbard. 1994. An improved rat hepatoma hybrid cell line. Generation and comparison with its hepatoma relatives and hepatocytes in vivo. *J. Cell Sci.* 107:813–825.

Shulman, J.M., R. Benton, and D. St Johnston. 2000. The *Drosophila* homolog of *C. elegans* PAR-1 organizes the oocyte cytoskeleton and directs oskar mRNA localization to the posterior pole. *Cell.* 101:377–388.

Sun, T.Q., B. Lu, J.J. Feng, C. Reinhard, Y.N. Jan, W.J. Fantl, and L.T. Williams. 2001. PAR-1 is a Dishevelled-associated kinase and a positive regulator of Wnt signalling. *Nat. Cell Biol.* 3:628–636.

Tomancak, P., F. Piano, V. Riechmann, K.C. Gunsalus, K.J. Kemphues, and A. Ephrussi. 2000. A *Drosophila melanogaster* homologue of *Caenorhabditis elegans* par-1 acts at an early step in embryonic-axis formation. *Nat. Cell Biol.* 2:458–460.

Tuma, P.L., L.K. Nyasae, and A.L. Hubbard. 2002. Nonpolarized cells selectively sort apical proteins from cell surface to a novel compartment, but lack apical retention mechanisms. *Mol. Biol. Cell.* 13:3400–3415.

Vaccari, T., and A. Ephrussi. 2002. The fusome and microtubules enrich Par-1 in the oocyte, where it effects polarization in conjunction with Par-3, BicD, Egl, and dynein. *Curr. Biol.* 12:1524–1528.

Vega-Salas, D.E., P.J. Salas, and E. Rodriguez-Boulan. 1987. Modulation of the expression of an apical plasma membrane protein of Madin-Darby canine kidney epithelial cells: cell–cell interactions control the appearance of a novel intracellular storage compartment. *J. Cell Biol.* 104:1249–1259.

Vega-Salas, D.E., P.J.I. Salas, and E. Rodriguez-Boulan. 1988. Exocytosis of vacuolar apical compartment (VAC): a cell–cell contact controlled mechanism for the establishment of the apical plasma membrane domain in epithelial cells. *J. Cell Biol.* 107:1717–1728.

Yap, A.S., and S.W. Manley. 2001. Microtubule integrity is essential for apical polarization and epithelial morphogenesis in the thyroid. *Cell Motil. Cytoskeleton.* 48:201–212.

Yeaman, C., K.K. Grindstaff, and W.J. Nelson. 1999. New perspectives on mechanisms involved in generating epithelial cell polarity. *Physiol. Rev.* 79:73–98.

Zegers, M.M., L.E. O'Brien, W. Yu, A. Datta, and K.E. Mostov. 2003. Epithelial polarity and tubulogenesis in vitro. *Trends Cell Biol.* 13:169–176.